Article

Multi-Responsive Eight-State Bis(acridinium-Zn(II) porphyrin) Receptor

Amy Edo-Osagie, Dylan Serillon, Federica Ruani, Xavier Barril, Christophe Gourlaouen, Nicola Armaroli,* Barbara Ventura,* Henri-Pierre Jacquot de Rouville,* and Valérie Heitz*

Read Online

ACCESS | Metrics & More | Article Recommendations | Supporting Information

ABSTRACT: A multi-responsive receptor consisting of two (acridinium-Zn(II) porphyrin) conjugates has been designed. The binding constant between this receptor and a ditopic guest has been modulated (i) upon addition of nucleophiles converting acridinium moieties into the non-aromatic acridane derivatives and (ii) upon oxidation of the porphyrin units. A total of eight states has been probed for this receptor resulting from the cascade of the recognition and responsive events. Moreover, the acridinium/ acridane conversion leads to a significant change of the photophysical properties, switching from electron to energy transfer processes. Interestingly, for the bis(acridinium-Zn(II) porphyrin) receptor, charge-transfer luminescence in the near-infrared has been observed.
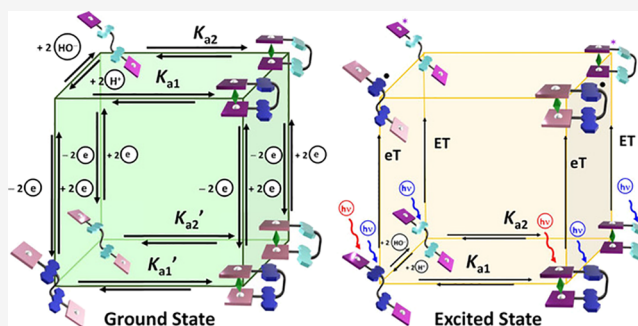
INTRODUCTION

Information processing and storage in biological structures relies on a network of complex systems. They interact with each other through various signaling events, resulting in modifications of their 3D structures and redox and electronic states. Simple synthetic systems using a binary-encoded molecule such as a molecular switch can provide the basis of information transmission in response to chemo-, electro-, or photostimulation.[1] Due to the robustness and diversity of such molecular components, their developments in the area of molecular computing, sensors, nanoreactors, machines, and motors have shown promise.[1d,2] Moreover, complex stimuli-responsive dynamics have been achieved using molecular systems that combine several responsive units.[3] On the other hand, a single multi-responsive molecular unit that gives rise to different output signals in response to different stimuli is attractive to reach advanced information processing with a low level of molecular components. Only few such units exist, such as spiropyrans, diarylethenes, dimethyldihydropyrenes, and flavyliums, that are light, redox, and/or thermally switchable but are mainly used as photoswitches.[4]

N-Substituted acridinium and porphyrin moieties represent appealing multi-responsive units that respond to chemical and redox signals by reversibly modifying their shape and/or their chemical and optical properties.[5,6] Their combination can lead to fast photoinduced electron transfer processes,[7] and their integration in various supramolecular systems gives rise to sensing and actuating properties.[6] Since the seminal work of Kubo and his group,[8] receptors pre-organizing porphyrin cores

coupled to secondary recognition units or switches also showed their ability to modulate their interaction with guests as the result of a large-amplitude motion.[9] Even if such a behavior was mainly triggered upon addition of metal cations,[10] neutral molecules,[11] and anions,[12] few examples involving light[13] as well as electron stimuli[14] were reported. Particularly, the group of Bucher[14] has developed a bis-(viologen-Zn(II) porphyrin) tweezer that is able to form a 1:1 host−guest complex with 1,4-diazabicyclo[2.2.2]octane (DABCO) ($K_a = 8.2 \times 10^4$ mol L^{-1}) upon formation of viologen π-dimers in dimethylformamide.

Herein, a tweezer consisting of two (acridinium-Zn(II) porphyrin) conjugates connected by a flexible linker was conceived to control the binding properties of the two porphyrins by various stimuli. The stimuli responsiveness of the system was investigated using three orthogonal stimuli (nucleophiles, electrons, and photons) to highlight the multi-state behavior of the tweezer.

RESULTS AND DISCUSSION

Design and Synthesis. The tweezer was designed with a long alkene chain connecting the two (acridinium-Zn(II)
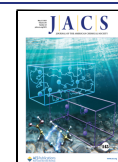
porphyrin) moieties to ensure enough flexibility to the system for coordination of a ditopic guest. Introduction of six *tert*-butyl groups was considered on the porphyrin moieties to increase their solubility. In addition, a short benzene linker was chosen to allow for electronic coupling in the acridinium-Zn(II) porphyrin conjugates.

The synthesis of the bis(acridinium-Zn(II) porphyrin) tweezer **1·2PF₆**, inspired by the work of Fukuzumi and co-workers,[7a] was performed in four synthetic steps starting from the commercially available 4-bromobenzaldehyde (Scheme 1).

Scheme 1. Synthesis of the Bis(acridinium-Zn(II) porphyrin) Tweezer 1·2PF₆
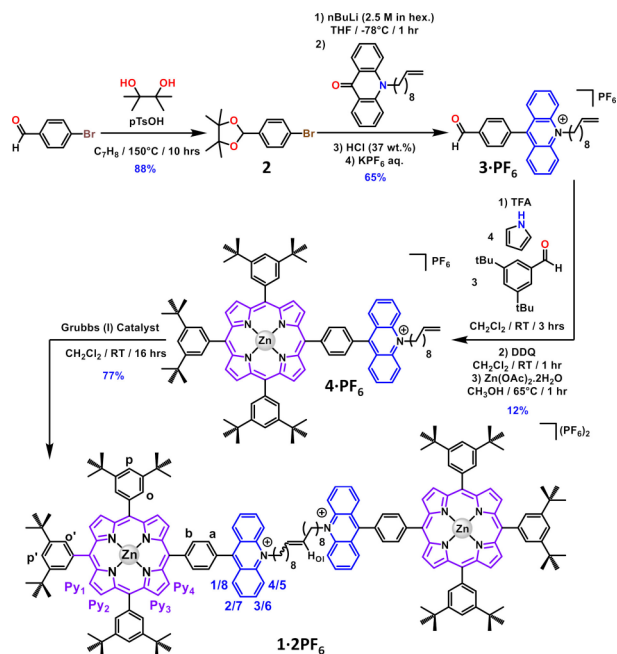
The aldehyde functional group was first protected by the reaction with 2,3-dimethylbutane-2,3-diol (1.1 equiv) in toluene.[15] The obtained 2-(4-bromophenyl)-4,4,5,5-tetramethyl-1,3-dioxolane (**2**) was reacted with nBuLi (1 equiv) in tetrahydrofuran at −78 °C followed by addition of dec-9-en-1-yl-acridin-9(10H)-one (1 equiv), obtained in one step as reported by us.[16] After acidification of the reaction mixture using HCl (37 wt %), the freshly formed 10-(dec-9-enyl)-9-(4-formylphenyl)acridin-10-ium chloride (**3·Cl**) was converted to the corresponding hexafluorophosphate salt (**3·PF₆**) by anion metathesis and isolated in 65% yield. The key intermediate **3·PF₆** was then reacted under Lindsey reaction conditions in the presence of pyrrole (4 equiv), 3,5-di-*tert*-butylbenzaldehyde (3 equiv),[17] and trifluoroacetic acid (TFA, 6 equiv) in CH₂Cl₂. After aromatization of the porphyrinogen using 2,3-dichloro-5,6-dicyano-1,4-benzoquinone (DDQ) (3 equiv), metalation of the free base porphyrins was undertaken using Zn(OAc)₂·2H₂O (1 equiv). After purification by column chromatography (SiO₂), the acridinium-Zn(II) porphyrin conjugate **4·PF₆** was isolated in 12% yield. Finally, the bis(acridinium-Zn(II) porphyrin) tweezer was formed from two molecules of **4·PF₆** under olefin metathesis conditions using the Grubbs I catalyst (10 mol %) in CH₂Cl₂.[18] The targeted tweezer **1·2PF₆** was obtained as a purple crystalline solid in 77% yield after purification by column chromatography followed by crystallization. Full characterization of the bis(acridinium-Zn(II)

porphyrin) tweezer **1·2PF₆** was performed by nuclear magnetic resonance (NMR) and UV/vis spectroscopies and by mass spectrometry (see Supporting Information).[19]

Binding Study. Nitrogenous ligands are known to bind Zn(II) porphyrins.[20] Thanks to the flexibility of the linker, the two remote Zn(II) porphyrins of the tweezer can adopt a face-to-face arrangement upon binding a ditopic ligand such as 4,4′-bipyridine (**4,4′-bipy**). The ^{1}H NMR spectrum (CD₂Cl₂, 298 K) of the 1:1 mixture of **1·2PF₆** and **4,4′-bipy** ($c = 1 \times 10^{-3}$ mol L^{-1}) revealed upfield shifts of all protons in comparison to the respective individual components, thus supporting the formation of the **4,4′-bipy ⊂ 1·2PF₆** host−guest complex (Figure 1). In particular, the most pronounced upfield shifts
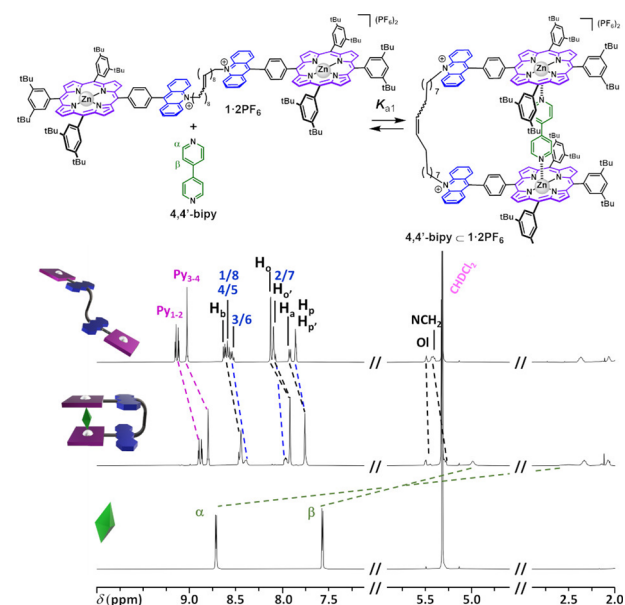

Figure 1. ^{1}H NMR (500 MHz, CD₂Cl₂, 298 K, $c = 1 \times 10^{-3}$ mol L^{-1}) stack of the bis(acridinium-Zn(II) porphyrin) tweezer **1·2PF₆** (top), the 1:1 complex **4,4′-bipy ⊂ 1·2PF₆** (middle), and **4,4′-bipy** (bottom).

were monitored for the H$_\alpha$ and H$_\beta$ protons of **4,4′-bipy** ($\Delta\delta(H_\alpha) = -6.25$ and $\Delta\delta(H_\beta) = -2.58$ ppm) due to the anisotropic ring current effect of the porphyrins (Figures S5.1−5.3). In addition, the pyrrolic protons of **1·2PF₆** experienced the influence of the coordination of the ditopic ligand ($\Delta\delta(Py_1) = -0.25$, $\Delta\delta(Py_2) = -0.25$, and $\Delta\delta(Py_{3-4}) = -0.23$ ppm). Interestingly, the acridinium protons were also upfield shifted ($\Delta\delta(H_{1/8}) = -0.15$, $\Delta\delta(H_{2/7}) = -0.13$, $\Delta\delta(H_{3/6}) = -0.14$, and $\Delta\delta(H_{4/5}) = -0.19$ ppm). In addition, diffusion-ordered spectroscopy (DOSY) experiments revealed an identical diffusion coefficient ($D = 380\ \mu m^2\ s^{-1}$) for the protons of **1·2PF₆** and **4,4′-bipy**, demonstrating the formation of the corresponding 1:1 host−guest complex (see Supporting Information, Figure S5.4). The estimated calculated hydrodynamic radius (R_H) considering a spherical host−guest system was found to be 13.2 Å. This value is identical to the value obtained for **1·2PF₆** (a diffusion coefficient of $D = 380\ \mu m^2\ s^{-1}$ corresponding to an R_H of 13.2 Å in a spherical model), confirming the discrete nature of **4,4′-bipy ⊂ 1·2PF₆**. Followed by UV/vis spectroscopy, titration experiments allowed the estimation of a binding constant of the 1:1 complex (K_{a1}) of $1.8 \pm 0.1 \times 10^5$ L mol^{-1} in CH₂Cl₂ (see Supporting Information, Figures S5.5−S5.6).[21] It is worthwhile

to note that the presence of an isosbestic point at 427 nm was observed upon titration, thus supporting the formation of a discrete species under dilute conditions ($c = 0.5 \times 10^{-5}$ mol L^{-1}) within a range below 20 equiv of **4,4′-bipy**. This hypothesis is corroborated by control titration experiments performed between the acridinium-Zn(II) porphyrin model compound **Acr⁺-ZnPorph·PF₆** and **4,4′-bipy** (see Supporting Information, Figures S5.13−S5.14). The corresponding (K_a) of $3.9 \pm 0.2 \times 10^3$ L mol^{-1} clearly demonstrates the cooperative binding of the ditopic **4,4′-bipy** ligand between both Zn(II) porphyrins of **1·2PF₆**.

Switching Properties and Binding and Fatigue Studies. The chemical switching properties of **1·2PF₆** were then investigated. Preparation of the bis-acridane derivative **5** was performed quantitatively upon addition of tetrabutylammonium hydroxide (TBAOH, 2.2 equiv, see Supporting Information). In the ^{1}H NMR spectrum of **5** (500 MHz, CD₂Cl₂, 298 K), dearomatization of the acridane units was confirmed by an observed upfield shift of the acridane protons ($\Delta\delta(H_{1/8}) = -0.97$, $\Delta\delta(H_{2/7}) = -0.72$, $\Delta\delta(H_{3/6}) = -1.16$, and $\Delta\delta(H_{4/5}) = -1.41$ ppm) in comparison to the ones of the acridinium units in **1·2PF₆** (see Supporting Information, Figures S4.1−4.2). It is worthwhile to note that a less pronounced upfield shift was also observed for the pyrrolic protons ($\Delta\delta(Py_1) = -0.21$, $\Delta\delta(Py_2) = -0.21$, and $\Delta\delta(Py_{3-4}) = -0.06$ ppm). In addition, hybridization change of the C_9 carbon from sp^2 in **1·2PF₆** to sp^3 in **5** was evidenced in the ^{13}C spectrum ($\Delta\delta(C_9) = -83.6$ ppm, Figure S4.3). UV/vis spectroscopy also supported the observed dearomatization in **5**. Indeed, upon formation of the acridane units in **1·2PF₆**, a decrease of the $\pi_A \to \pi_A$* acridinium-centered transitions at 349 nm ($\varepsilon = 38,000$ L mol^{-1} cm^{-1}) and 363 nm (55,850 L mol^{-1} cm^{-1}) as well as the combination with a porphyrin → acridinium charge-transfer (CT) transition at 458 nm (25,800 L mol^{-1} cm^{-1}) was monitored (Figure 2). In addition, the CT transition above 600 nm disappears upon conversion (the calculated UV/vis spectra are in accordance with the existence of a CT band at low energy, (Figure S7.2). The reversible interconversion between **1·2PF₆** and **5** was established upon addition of TFA (2.2 equiv). It is worthwhile to note that no demetalation of the porphyrin cores was observed, as shown by the fatigue study followed by UV/vis spectroscopy (Figure 2, inset).

The ability of the bis-acridane receptor **5** to bind **4,4′-bipy** was also studied by NMR and UV/vis spectroscopies. As previously seen for **1·2PF₆**, ^{1}H NMR experiments of a 1:1 mixture of **4,4′-bipy** and **5** revealed that the pyrrolic protons ($\Delta\delta(Py_1) = -0.21$, $\Delta\delta(Py_2) = -0.19$, and $\Delta\delta(Py_{3-4}) = -0.21$ ppm) and the H_α and H_β protons ($\Delta\delta(H_\alpha) = -6.38$ and $\Delta\delta(H_\beta) = -2.71$ ppm) were the most affected (see Supporting Information, Figures S5.7−5.8). In comparison, the acridane units ($\Delta\delta(H_{1/8}) = -0.06$, $\Delta\delta(H_{2/7}) = -0.04$, $\Delta\delta(H_{3/6}) = -0.01$, and $\Delta\delta(H_{4/5}) = -0.01$ ppm) were almost not affected. As expected, the sp^3 hybridization of the C_9 atom in **5** precludes electronic coupling between both porphyrin and acridane units. DOSY experiments also confirmed the formation of the 1:1 host−guest complex since all protons of **5** and **4,4′-bipy** correspond to **4,4′-bipy ⊂ 5** as a single diffusing species ($D = 405$ µm^2 s^{-1}, Figure S5.10). The estimated R_H (12.4 Å) was in a similar range to that of the **4,4′-bipy ⊂ 1·2PF₆** complex. Finally, a decrease of ca. 25% of the binding constant of **4,4′-bipy** with **5** ($K_{a2} = 1.4 \pm 0.3 \times 10^5$
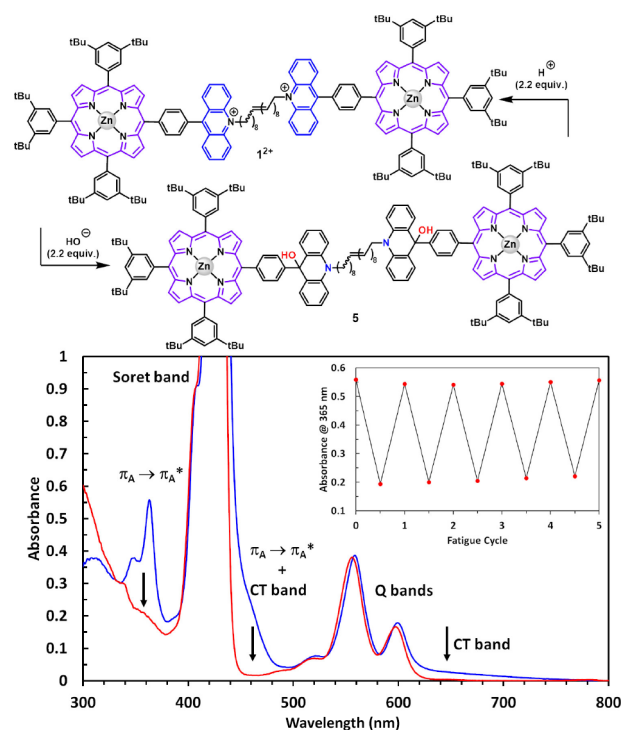
**Figure 2.** UV/vis (CH₂Cl₂, $l = 0.1$ cm, 298 K) spectra of a solution of **1·2PF₆** ($c = 1 \times 10^{-4}$ mol L^{-1}) before (blue) and after addition of TBAOH (2.2 equiv, red). Inset: fatigue study monitored by UV/vis spectroscopy at 363 nm. Each cycle corresponds to the successive addition of TBAOH (2.2 equiv) followed by addition of TFA (2.2 equiv).

L mol^{-1} in CH₂Cl₂) compared to **1·2PF₆** was estimated by UV/Vis spectroscopy (Figures S5.11−S5.12).[22]

To gain further insights on the binding of **4,4′-bipy** to the receptors **1·2PF₆** and **5**, molecular dynamics simulations were performed in explicit CH₂Cl₂. Conformational clustering was determined by K-nearest neighbors (Knn) clustering based on atomic root-mean-square deviation[23] between conformations.[24] Clustering quality was supported by satisfying the Davies−Bouldin index and pseudo-F statistic values (see ESI, Table S9.1). Conformation clusters highlight the preferential open and semi-open conformations both for **1·2PF₆** and **5** (Figures S9.2−S9.3), although the former has a greater preference for extended conformations, whereas the latter presents a larger variety of conformations as it lacks charge repulsion between the acridinium units. It is worthwhile to note that the calculated R_g values from representative geometries extracted from the Knn analysis (Table S9.2 and Figures S9.2−S9.5) are in good agreement with the experimental estimated R_H values (Figures S9.6−S9.7). Computational prediction of binding free energies was obtained on a conformational sampling. Predicted binding free energies for **4,4′-bipy ⊂ 5** and **4,4′-bipy ⊂ 1·2PF₆** were very close to the experimental ones ($\Delta(\Delta G) = +0.29$ and -0.11 kcal mol^{-1}, respectively, Figure 3).[25]

Electrochemical Study. The tweezer **1·2PF₆** exhibits a quasi-reversible oxidation process ($E_{1/2}^{(1)}$) at 0.750 V vs saturated calomel electrode (SCE) and a quasi-reversible reduction process ($E_{1/2}^{(2)}$) at -0.535 V vs SCE in C₂H₄Cl₂ (Figure 4). Each process corresponds, respectively, to the oxidation of both porphyrin moieties and the reduction of both acridinium moieties.[26] The bis-acridane tweezer **5** shows only
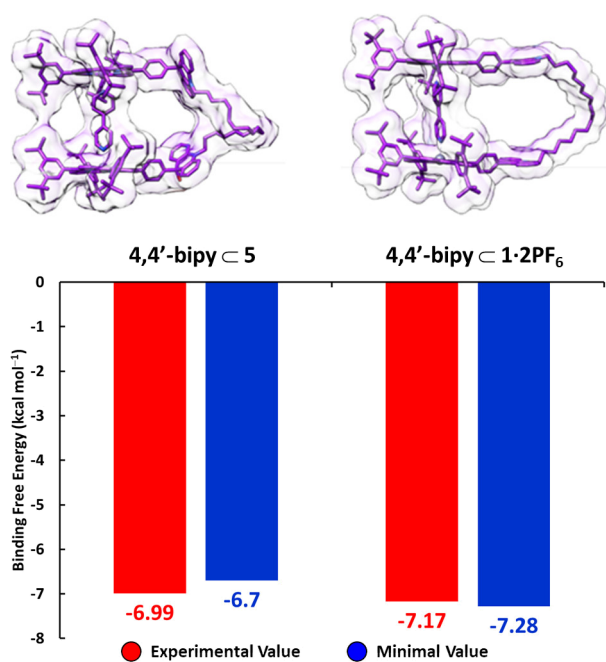
Figure 3. Comparison of the experimental and predicted binding free energy of **4,4′-bipy ⊂ 5** and **4,4′-bipy ⊂ 1·2PF$_6$**.
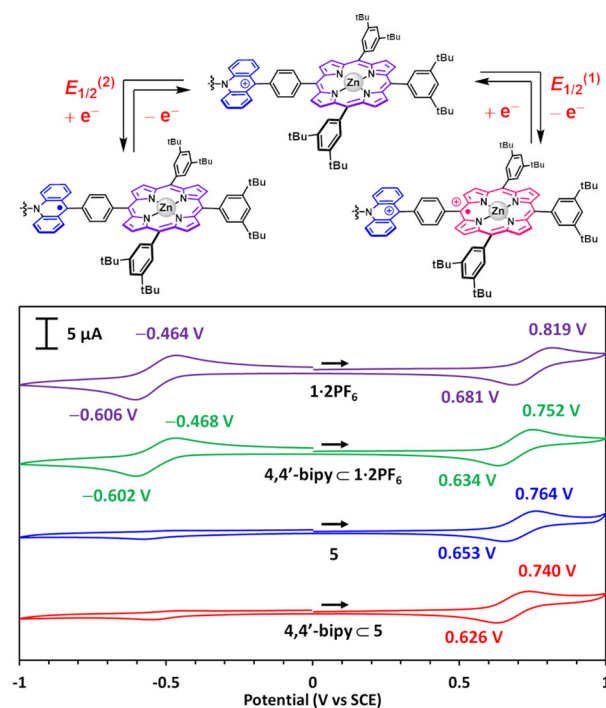
Figure 4. Cyclic voltammograms (C$_2$H$_4$Cl$_2$, WE: Pt, CE: Pt, RE: SCE, 100 mV s^{-1}, TBAPF$_6$ 0.1 mol L^{-1}) of a solution of **1·2PF$_6$** ($c = 1 \times 10^{-3}$ mol L^{-1}) before (purple) and after addition of 1 equiv of **4,4′-bipy** (green) and a solution of **5** ($c = 1 \times 10^{-3}$ mol L^{-1}) before (blue) and after addition of 1 equiv of **4,4′-bipy** (red).

the oxidation process of porphyrins ($E_{1/2}^{(1)}$) at 0.708 V vs SCE.[27] The disappearance of the reduction process in **5** in comparison to **1·2PF$_6$** reflects the dearomatization of the acridinium units. This dearomatization leads to a cathodic shift of 42 mV of the oxidation potential since the porphyrins connected to the acridane moieties are less electron-deficient than those linked to the acridinium moieties. This observation

supports the occurrence of an electronic coupling between the porphyrin and the acridinium units.

Upon addition of **4,4′-bipy** (1 equiv corresponding to 88% complex formation for both receptors), a cathodic shift for the oxidation potential of **1·2PF$_6$** and **5** and no modifications in the reduction range were observed. This observation supports the binding of the ditopic ligand between both porphyrins in **1·2PF$_6$** and **5**. In addition, coordination of **4,4′-bipy** increases the electronic density of the Zn(II) porphyrin units, making them easier to oxidize. The half-wave potential difference before and after addition of **4,4′-bipy** ($\Delta E_{1/2} = -57$ mV in **1·2PF$_6$** and $\Delta E_{1/2} = -25$ mV in **5**) allows the estimation of the binding constants K_{a1}' of 1.9×10^3 L mol^{-1} for **4,4′-bipy ⊂ [1·2PF$_6$]$^{2(\cdot+)}$** and K_{a2}' of 1.9×10^4 L mol^{-1} for **4,4′-bipy ⊂ [5]$^{2(\cdot+)}$**, respectively (Table 1).[16,28] These binding constants

Table 1. Measured Redox Potentials (V vs SCE) of 1·2PF$_6$, 4,4′-bipy ⊂ 1·2PF$_6$, 5, and 4,4′-bipy ⊂ 5 and the Corresponding $E_{1/2}$ (V vs SCE), Binding Constants K_a and K_a' (L mol^{-1}), and HOMO−LUMO Energies (eV)

| compound	1·2PF$_6$	Bipy ⊂ 1·2PF$_6$	5	Bipy ⊂ 5
$E_{1/2}^{(1)}$	+0.750	+0.693	+0.708	+0.683
$E_{1/2}^{(2)}$	−0.535	−0.535		
K_a		1.8×10^5		1.4×10^5
$K_a'^{a}$		1.9×10^3		1.9×10^4
HOMO (eV)	−5.85	−5.63	−5.66	−5.40
LUMO (eV)	−3.94	−3.93	−2.81	−2.69

^{a}Binding constant estimated after oxidation of the porphyrins in the tweezers.

evidence that the host−guest association between the receptors and **4,4′-bipy** can be electrochemically controlled according to the redox state of the porphyrin core. In addition, the acridinium units act as a remote site to modulate the binding affinity between the porphyrin fragments and the ditopic ligand. This remote control can be rationalized by the electronic coupling existing between the porphyrin and the acridinium cores in the tweezer **1·2PF$_6$**. It enhances the Lewis acidity of the Zn(II) porphyrins, thus strengthening the binding to **4,4′-bipy**.

In order to gain further insight on the observed electrochemical behavior of **1·2PF$_6$** and **5**, density functional theory (DFT) calculations were undertaken on models consisting of acridinium-Zn(II) porphyrin (**Acr⁺-ZnPorph**) and acridane-Zn(II) porphyrin (**Acr(OH)-ZnPorph**) conjugates (see Supporting Information, Scheme S7.1). This simplification is justified since no electronic coupling exists between both of the acridinium-Zn(II) porphyrin conjugates in **1·2PF$_6$** and **5**. For **Acr⁺-ZnPorph**, the HOMO ($E_{\mathrm{HOMO}} = -5.85$ eV) and LUMO ($E_{\mathrm{LUMO}} = -3.94$ eV) frontier orbitals are localized on the porphyrin and the acridinium cores, respectively, as expected (Tables S7.1−S7.2). In **Acr(OH)-ZnPorph**, the highest occupied molecular orbital (HOMO, $E_{\mathrm{HOMO}} = -5.66$ eV) and the lowest unoccupied molecular orbital (LUMO, $E_{\mathrm{LUMO}} = -2.81$ eV) are both localized on the porphyrin cores and are higher in energy than in **Acr⁺-ZnPorph**. This is in good agreement with the lower oxidation potential and the absence of the reduction process in **5** compared to **1·2PF$_6$** in the same electrochemical range (Tables S7.1 and S7.4). The influence of **4,4′-bipy** was simulated by the coordination of pyridine to the Zn(II) porphyrin. Upon complexation, the HOMO is destabilized in both adducts (+0.22 and +0.26 eV for **Acr⁺-**

ZnPorph and **Acr(OH)-ZnPorph** conjugates, respectively, Tables S7.3 and S7.5), thus explaining the observed cathodic shift in the **4,4′-bipy ⊂ 1·2PF$_6$** and the **4,4′-bipy ⊂ 5** complexes.

Altogether, these results demonstrate that the present molecular system is able to reach eight distinct states by combining chemical (hydroxide ions and a ditopic ligand) and electrochemical stimuli. This behavior can be illustrated with a cubic scheme for which each apex is a state of the tweezer (Figure 5). The three dimensions of the cube represent the different orthogonal stimuli.
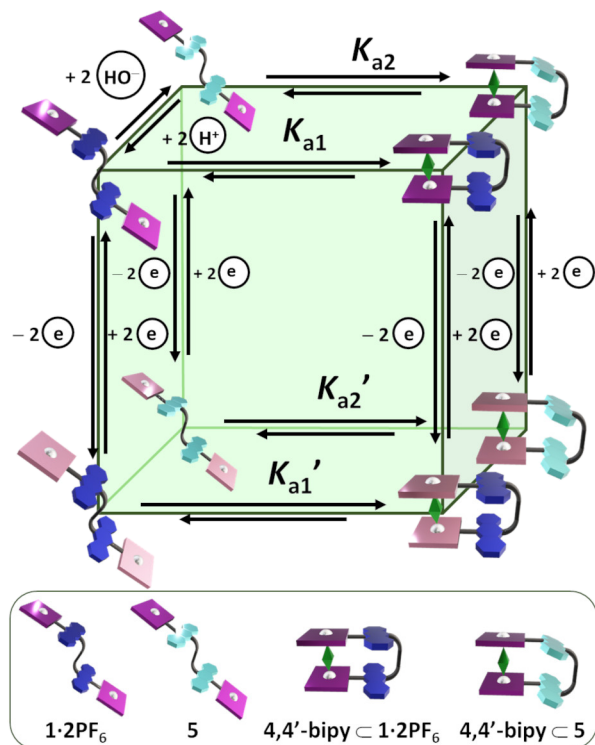

Figure 5. Cubic scheme showing the eight different states of **1·2PF$_6$** upon addition of **4,4′-bipy**, nucleophiles, and electrons.

Photophysical Studies. Investigations of the excited-state dynamics of both receptors **1·2PF$_6$** and **5** were also performed and revealed remarkably different behaviors.

First, **1·2PF$_6$** was proved to be poorly emissive in CH$_2$Cl$_2$ ($\Phi_{fl} < 10^{-4}$) regardless of the excited chromophore, porphyrin or acridinium (Figures 6, S8.3, and Table S8.1). The excitation spectrum of **1·2PF$_6$** (at $\lambda_{em} = 648$ nm, corresponding to the emission of the porphyrin moiety) revealed the same absorption features of the Zn(II) tetraphenylporphyrin model compound (Figure S8.5) and the absence of the absorption bands of the acridinium moiety at 349 and 363 nm. These observations indicate that no energy transfer occurs from the acridinium to the porphyrin core in **1·2PF$_6$**, thus suggesting that the quenching results from an ultrafast electron transfer process. This hypothesis was supported by transient absorption analysis with fs resolution (Figures 7a and S8.12b). Excitation of either the porphyrin or the acridinium moieties resulted in ultrafast formation (0.6 ps) of an envelope of bands between 600 and 700 nm and a peak at 410 nm, assigned to the Zn(II) porphyrin cation, as well as transitions at 480 and 520 nm attributed to the reduced acridinium units.[26,29] These changes reflect the formation of a charge-separated (CS) state
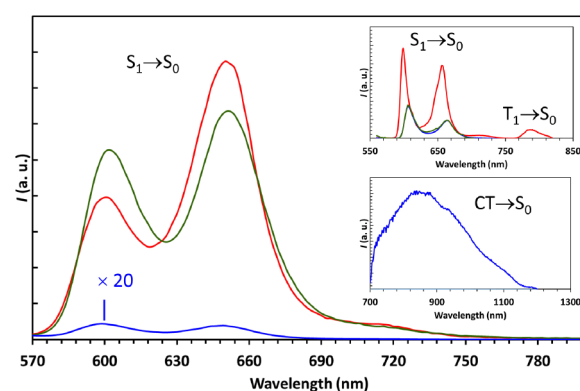
Figure 6. Corrected fluorescence spectra of isoabsorbing solutions ($A = 0.12$) of the model compound Zn(II) tetraphenylporphyrin (red), **1·2PF$_6$** (blue), and **5** (green) at RT in CH$_2$Cl$_2$ or at 77 K in CH$_2$Cl$_2$:CH$_3$OH (1:1) (top inset) upon selective excitation of the porphyrin moiety ($\lambda_{exc} = 550$ nm). In the bottom inset is reported the near-infrared corrected emission spectrum of **1·2PF$_6$** in toluene (CT luminescence, $\lambda_{exc} = 550$ nm).
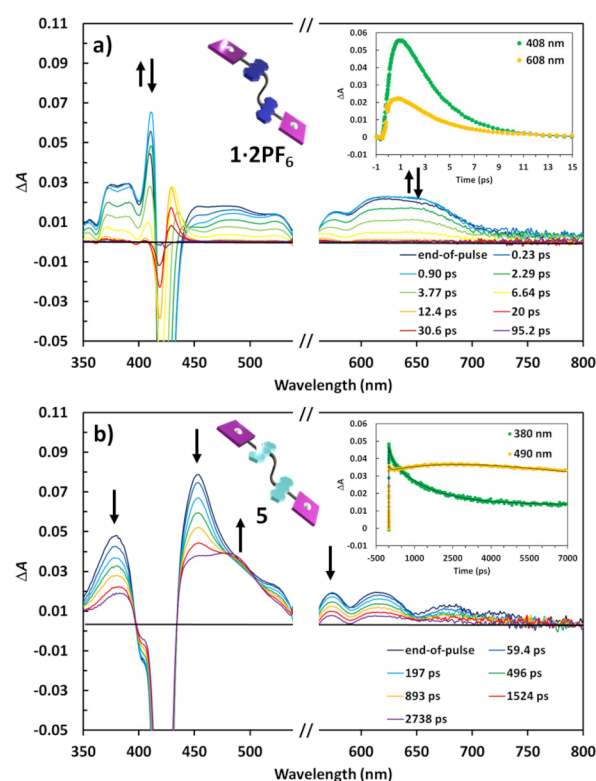
Figure 7. Transient absorption spectra of (a) **1·2PF$_6$** and (b) **5** in CH$_2$Cl$_2$ at different delays. Excitation at 550 nm ($A_{550} = 0.1$, 0.2 cm optical path, 4 μJ/pulse). Insets: ΔA time evolutions (dots) and fittings (lines) at the indicated wavelengths.

involving a photoinduced electron transfer from a porphyrin to an acridinium moiety followed by a fast charge recombination of the order of 3 ps. Interestingly, the porphyrin fluorescence in **1·2PF$_6$** was recovered in a rigid matrix at 77 K (Figure 6, top inset), where solvent reorganization is disfavored, and thus, the charge separation process does not occur.

Remarkably, in toluene and regardless of the excitation wavelength of **1·2PF$_6$**, a broad luminescence band in the near-infrared region peaking at 856 nm was observed (Figure 6, bottom inset, and Figure S8.9).[30] This band can be ascribed to

porphyrin → acridinium CT luminescence. Such a luminescence is rarely observed and has been similarly reported for porphyrin/fullerene,[31] porphyrin/anthracene,[32] or porphyrin/anthraquinone[33] donor−acceptor systems. The energy of the related CT state in **1·2PF$_6$** (E_{CT} = 1.45 eV) corresponds to the CS state in toluene (Figure S8.19), thus underpinning a radiative charge recombination process.

In contrast to **1·2PF$_6$**, no emission quenching was observed for the Zn(II) porphyrin units in **5** (λ_{max} = 600, 650 nm; Φ_{fl} = 0.036, τ = 1.7 ns at RT), and the same behavior was maintained at 77 K (Figure 6 and Table S8.1). Moreover, upon prevalent excitation of the acridane moieties at 292 nm, no residual acridane fluorescence was detected. Instead, a 95% sensitization of the porphyrin emission was monitored (Figure S8.4), thus suggesting an almost quantitative energy transfer from the acridane to the porphyrin component. Further evidence was provided by the excitation spectrum collected at 670 nm being in good agreement with the absorption transitions of both the porphyrin and the acridane moieties (Figure S8.6). Upon selective excitation of the porphyrin unit at 550 nm, ultrafast transient absorption experiments revealed for **5** a spectral evolution attributable to S$_1$ → T$_1$ intersystem crossing (Figure 7b, fitted lifetime: 1.7 ns), as observed for the model Zn(II) tetraphenylporphyrin (Figure S8.10).

Solutions of **1·2PF$_6$** (c = 2.1 × 10^{-6} mol L^{-1}) and **5** (c = 2.5 × 10^{-6} mol L^{-1}) in the presence of **4,4′-bipy** (c = 1.0 × 10^{-3} mol L^{-1}) were also prepared in CH$_2$Cl$_2$. Upon excitation of the complex **4,4′-bipy ⊂ 1·2PF$_6$** in the Q-band region (λ_{exc} = 558 nm), the already weak emission of **1·2PF$_6$** was further reduced (Figure S8.15). Transient absorption spectra were recorded upon excitation of the porphyrin components in **4,4′-bipy ⊂ 1·2PF$_6$** at 550 nm. These experiments corroborated the previously observed electron transfer in **1·2PF$_6$**. However, slightly faster kinetics compared to the free conjugate were observed (charge separation of 0.5 ps and recombination occurring in 2.3 ps; Figure S8.17a). On the other hand, the emission of the complex **4,4′-bipy ⊂ 5** appeared red-shifted and slightly decreased with respect to that of the receptor **5** alone (Figure S8.16). The emission quantum yield (0.023) and lifetime (1.1 ns) of the Zn(II) porphyrin moieties suggest some electronic interactions with **4,4′-bipy**. Transient absorption spectra of **4,4′-bipy ⊂ 5** showed the typical intersystem crossing pattern of the Zn(II) porphyrin units with a lifetime for the singlet decay and triplet rise in line with that observed in luminescence measurements (1.1 ns, Figure S8.17b).

Overall, the complexation with **4,4′-bipy** slightly affects the photophysical properties of the individual receptors **1·2PF$_6$** and **5**. Conversely, hydroxide ions as chemical stimuli strongly affect the photophysical properties of the tweezer that switch from an ultrafast photoinduced electron transfer from the porphyrin to the acridinium in **1·2PF$_6$** to an almost quantitative energy transfer from the acridane to the porphyrin in **5** (Figure 8).

CONCLUSIONS

The synthesis of a bis(acridinium-Zn(II) porphyrin) receptor was successfully described. The efficient binding of **4,4′-bipy** by the Zn(II) porphyrin units of the receptor was demonstrated. This receptor was also proved to have switching properties. Upon addition of hydroxide anions, the acridinium moieties were converted to their corresponding acridane derivatives in a quantitative manner. This strongly modifies
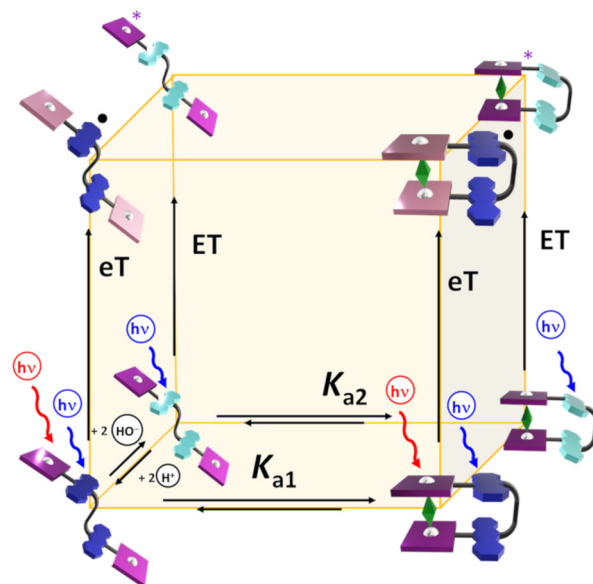
Figure 8. Cubic scheme showing the photoinduced processes of **1·2PF$_6$** and **5** and their corresponding **4,4′-bipy** complexes (eT, electron transfer; ET, energy transfer; and asterisk, porphyrin singlet excited state).

the excited-state behavior of the tweezer, allowing the switching from a system converting UV/visible light into charge separation to a system that harvests and emits light. The same chemical input led also to the modulation of the host−guest interaction, resulting in a 25% decrease of the corresponding association constant. The ditopic ligand and hydroxide anions have been shown to act as orthogonal stimuli on the tweezer, both modifying the oxidation potential of the porphyrin cores. The binding and the switching properties of this bis(acridinium-Zn(II) porphyrin) receptor gave rise to eight distinct states, best represented as a cubic scheme. This work shows that porphyrin units coupled to acridinium cores are promising aromatic conjugates for the development of multi-state molecular systems and allosteric receptors.

ASSOCIATED CONTENT

Ⓢ Supporting Information

The Supporting Information is available free of charge at https://pubs.acs.org/doi/10.1021/jacs.3c01089.

Synthesis procedures, NMR spectra, absorption and emission spectra, electrochemical and photophysical data, and DFT calculations (PDF)

AUTHOR INFORMATION

Corresponding Authors

Nicola Armaroli − *Istituto per la Sintesi Organica e la Fotoreattività (ISOF), Consiglio Nazionale delle Ricerche (CNR), Bologna 40129, Italy;* ⓘ orcid.org/0000-0001-8599-0901; Email: nicola.armaroli@isof.cnr.it

Barbara Ventura − *Istituto per la Sintesi Organica e la Fotoreattività (ISOF), Consiglio Nazionale delle Ricerche (CNR), Bologna 40129, Italy;* ⓘ orcid.org/0000-0002-8207-1659; Email: barbara.ventura@isof.cnr.it

Henri-Pierre Jacquot de Rouville − *Laboratoire de Synthèse des Assemblages Moléculaires Multifonctionnels, Institut de Chimie de Strasbourg, CNRS/UMR 7177, 67000 Strasbourg, France;* Email: hpjacquot@unistra.fr

Valérie Heitz − *Laboratoire de Synthèse des Assemblages Moléculaires Multifonctionnels, Institut de Chimie de Strasbourg, CNRS/UMR 7177, 67000 Strasbourg, France;* ⓘ orcid.org/0000-0002-5828-9199; Email: v.heitz@unistra.fr

Authors

Amy Edo-Osagie − *Laboratoire de Synthèse des Assemblages Moléculaires Multifonctionnels, Institut de Chimie de Strasbourg, CNRS/UMR 7177, 67000 Strasbourg, France;* ⓘ orcid.org/0000-0003-4985-8350

Dylan Serillon − *Departament de Farmacia i Tecnología Farmaceutica, i Fisicoquímica, Institut de Biomedicina (IBUB), Universitat de Barcelona, E-08028 Barcelona, Spain*

Federica Ruani − *Istituto per la Sintesi Organica e la Fotoreattività (ISOF), Consiglio Nazionale delle Ricerche (CNR), Bologna 40129, Italy*

Xavier Barril − *Departament de Farmacia i Tecnología Farmaceutica, i Fisicoquímica, Institut de Biomedicina (IBUB), Universitat de Barcelona, E-08028 Barcelona, Spain; Catalan Institution for Research and Advanced Studies (ICREA), Barcelona 08010, Spain;* ⓘ orcid.org/0000-0002-0281-1347

Christophe Gourlaouen − *Laboratoire de Chimie Quantique, Institut de Chimie de Strasbourg, CNRS/UMR 7177, 67000 Strasbourg, France*

Complete contact information is available at:
https://pubs.acs.org/10.1021/jacs.3c01089

Notes

The authors declare no competing financial interest.

■ REFERENCES

(1) (a) de Silva, A. P.; Gunaratne, H. Q. N.; McCoy, C. P. A molecular photoionic AND gate based on fluorescent signalling. *Nature* **1993**, *364*, 42−44. (b) de Silva, A. P.; Gunaratne, H. Q. N.; Gunnlaugsson, T.; Huxley, A. J. M.; McCoy, C. P.; Rademacher, J. T.; Rice, T. E. Signaling Recognition Events with Fluorescent Sensors and Switches. *Chem. Rev.* **1997**, *97*, 1515−1566. (c) de Silva, A. P.; McClenaghan, N. D. Molecular-Scale Logic Gates. *Chem. − Eur. J.* **2004**, *10*, 574−586. (d) Feringa, B. L.; Browne, W. R. (Eds. *Molecular Switches*, 2nd ed.); Wiley-VCH: Weinheim, Germany, 2011.

(2) (a) Kassem, S.; van Leeuwen, T.; Lubbe, A. S.; Wilson, M. R.; Feringa, B. L.; Leigh, D. A. Artificial molecular motors. *Chem. Soc. Rev.* **2017**, *46*, 2592−2621. (b) Diaz-Moscoso, A.; Ballester, P. Light-responsive molecular containers. *Chem. Commun.* **2017**, *53*, 4635−4652. (c) Park, J. S.; Sessler, J. L. Tetrathiafulvalene (TTF)-Annulated Calix[4]pyrroles: Chemically Switchable Systems with Encodable Allosteric Recognition and Logic Gate Functions. *Acc. Chem. Res.* **2018**, *51*, 2400−2410. (d) Martynov, A. G.; Safonova, E. A.; Tsivadze, A. Y.; Gorbunova, Y. G. Functional molecular switches involving tetrapyrrolic macrocycles. *Coord. Chem. Rev.* **2019**, *387*,

325−347. (e) Milić, J. V.; Diederich, F. The Quest for Molecular Grippers: Photo-Electric Control of Molecular Gripping Machinery. *Chem. − Eur. J.* **2019**, *25*, 8440−8452. (f) Goswami, A.; Saha, S.; Biswas, P. K.; Schmittel, M. (Nano)mechanical Motion Triggered by Metal Coordination: from Functional Devices to Networked Multicomponent Catalytic Machinery. *Chem. Rev.* **2020**, *120*, 125−199. (g) Dattler, D.; Fuks, G.; Heiser, J.; Moulin, E.; Perrot, A.; Yao, X.; Giuseppone, N. Design of Collective Motions from Synthetic Molecular Switches, Rotors, and Motors. *Chem. Rev.* **2020**, *120*, 310−433.

(3) (a) Funeriu, D. P.; Lehn, J.-M.; Fromm, K. M.; Fenske, D. Multiple Expression of Molecular Information: Enforced Generation of Different Supramolecular Inorganic Architectures by Processing of the Same Ligand Information through Specific Coordination Algorithms. *Chem. − Eur. J.* **2000**, *6*, 2103−2111. (b) Goodman, A.; Breinlinger, E.; Ober, M.; Rotello, V. M. Controlled Multi-Stage Recognition of Guests Using Orthogonal Electro- and Photochemical Inputs. *J. Am. Chem. Soc.* **2001**, *123*, 6213−6214. (c) Szalóki, G.; Sevez, G.; Berthet, J.; Pozzo, J.-L.; Delbaere, S. A Simple Molecule-Based Octastate Switch. *J. Am. Chem. Soc.* **2014**, *136*, 13510−13513. (d) Gaikwad, S.; Goswami, A.; De, S.; Schmittel, M. A Metal-loregulated Four-State Nanoswitch Controls Two-Step Sequential Catalysis in an Eleven-Component System. *Angew. Chem., Int. Ed.* **2016**, *55*, 10512−10517. (e) Doistau, B.; Benda, L.; Cantin, J.-L.; Chamoreau, L.-M.; Ruiz, E.; Marvaud, V.; Hasenknopf, B.; Vives, G. Six States Switching of Redox-Active Molecular Tweezers by Three Orthogonal Stimuli. *J. Am. Chem. Soc.* **2017**, *139*, 9213−9220. (f) Rabelo, R.; Stiriba, S.-E.; Cangussu, D.; Pereira, C. L. M.; Moliner, N.; Ruiz-García, R.; Cano, J.; Faus, J.; Journaux, Y.; Julve, M. When Molecular Magnetism Meets Supramolecular Chemistry: Multifunctional and Multiresponsive Dicopper(II) Metallacyclophanes as Proof-of-Concept for Single-Molecule Spintronics and Quantum Computing Technologies? *Magnetochemistry* **2020**, *6*, 69.

(4) (a) Klajn, R. Spiropyran-based dynamic materials. *Chem. Soc. Rev.* **2014**, *43*, 148−184. (b) Steen, J. D.; Duijnstee, D. R.; Sardjan, A. S.; Martinelli, J.; Kortekaas, L.; Jacquemin, D.; Browne, W. R. Electrochemical Ring-Opening and -Closing of a Spiropyran. *J. Phys. Chem. A* **2021**, *125*, 3355−3361. (c) Gilat, S. L.; Kawai, S. H.; Lehn, J.-M. Light-Triggered Molecular Devices: Photochemical Switching Of optical and Electrochemical Properties in Molecular Wire Type Diarylethene Species. *Chem. − Eur. J.* **1995**, *1*, 275−284. (d) Cobo, S.; Lafolet, F.; Saint-Aman, E.; Philouze, C.; Bucher, C.; Silvi, S.; Credi, A.; Royal, G. Reactivity of a pyridinium-substituted dimethyldihydropyrene switch under aerobic conditions: self-sensitized photo-oxygenation and thermal release of singlet oxygen. *Chem. Commun.* **2015**, *51*, 13886−13889. (e) Moncelsi, G.; Ballester, P. Photoswitchable Host-Guest Systems Incorporating Hemithioindigo and Spiropyran Units. *ChemPhotoChem* **2019**, *3*, 304−317. (f) Pina, F.; Melo, M. J.; Laia, C. A. T.; Parola, A. J.; Lima, J. C. Chemistry and applications of flavylium compounds: a handful of colours. *Chem. Soc. Rev.* **2012**, *41*, 869−908.

(5) (a) Kurihara, K.; Yazaki, K.; Akita, M.; Yoshizawa, M. A Switchable Open/closed Polyaromatic Macrocycle that Shows Reversible Binding of Long Hydrophilic Molecules. *Angew. Chem., Int. Ed.* **2017**, *56*, 11360−11364. (b) Gosset, A.; Xu, Z.; Maurel, F.; Chamoreau, L.-M.; Nowak, S.; Vives, G.; Perruchot, C.; Heitz, V.; Jacquot de Rouville, H.-P. A chemically-responsive bis-acridinium receptor. *New J. Chem.* **2018**, *42*, 4728−4734. (c) Jacquot de Rouville, H.-P.; Hu, J.; Heitz, V. N-Substituted Acridinium as a Multi-Responsive Recognition Unit in Supramolecular Chemistry. *ChemPlusChem* **2021**, *86*, 110−129. (d) Hu, J.; Adrouche, S.; Gauthier, E. S.; Le Breton, N.; Cecchini, M.; Gourlaouen, C.; Choua, S.; Heitz, V.; Jacquot de Rouville, H.-P. Dual Read-out of the Mechanical Response of a Bis-acridinium [2]Rotaxane. *Chem. − Eur. J.* **2022**, *28*, No. e202202840.

(6) (a) Mizutani, T.; Wada, K.; Kitagawa, S. Molecular Recognition of DNA Intercalators at Nanomolar Concentration in Water. *J. Am. Chem. Soc.* **2001**, *123*, 6459−6460. (b) Wada, K.; Mizutani, T.; Matsuoka, H.; Kitagawa, S. A New Strategy for the Design of Water-

Soluble Synthetic Receptors: Specific Recognition of DNA Intercalators and Diamines. *Chem. − Eur. J.* **2003**, *9*, 2368−2380. (c) Tanaka, M.; Ohkubo, K.; Gros, C. P.; Guilard, R.; Fukuzumi, S. Persistent Electron-Transfer State of a π-Complex of Acridinium Ion Inserted between Porphyrin Rings of Cofacial Bisporphyrins. *J. Am. Chem. Soc.* **2006**, *128*, 14625−14633. (d) Chaudhary, A.; Rath, S. P. Encapsulation of TCNQ and the Acridinium Ion within a Bisporphyrin Cavity: Synthesis, Structure, and Photophysical and HOMO−LUMO-Gap-Mediated Electron-Transfer Properties. *Chem. − Eur. J.* **2012**, *18*, 7404−7417. (e) Kim, D.; Lee, S.; Gao, G.; Kang, H. S.; Ko, J. A molecular-clip-based approach to cofacial zinc−porphyrin complexes. *J. Organomet. Chem.* **2010**, *695*, 111−119.

(7) (a) Kotani, H.; Ohkubo, K.; Crossley, M. J.; Fukuzumi, S. An Efficient Fluorescence Sensor for Superoxide with an Acridinium Ion-Linked Porphyrin Triad. *J. Am. Chem. Soc.* **2011**, *133*, 11092−11095. (b) Edo-Osagie, A.; Sánchez-Resa, D.; Serillon, D.; Bandini, E.; Gourlaouen, C.; Jacquot de Rouville, H.-P.; Ventura, B.; Heitz, V. Synthesis, electronic and photophysical properties of a bisacridinium-Zn(II) porphyrin conjugate. *C. R. Chim.* **2021**, *24*, 47−55.

(8) (a) Kubo, Y.; Murai, Y.; Yamanaka, J.-I.; Tokita, S.; Ishimaru, Y. A new biphenyl-20-crown-6-derived zinc(II) porphyrin dimer with a potentially heterotropic allostery. *Tetrahedron Lett.* **1999**, *40*, 6019−6023. (b) Kubo, Y.; Ohno, T.; Yamanaka, J.; Tokita, S.; Iida, T.; Ishimaru, Y. Chirality-Transfer Control Using a Heterotopic Zinc(II) Porphyrin Dimer. *J. Am. Chem. Soc.* **2001**, *123*, 12700−12701.

(9) (a) Beletskaya, I.; Tyurin, V. S.; Tsivadze, A. Y.; Guilard, R.; Stern, C. Supramolecular Chemistry of Metalloporphyrins. *Chem. Rev.* **2009**, *109*, 1659−1713. (b) Valderreya, V.; Aragaya, G.; Ballester, P. Porphyrin tweezer receptors: Binding studies, conformational properties and applications. *Coord. Chem. Rev.* **2014**, *258-259*, 137−156. (c) Durot, S.; Taesch, T.; Heitz, V. Multiporphyrinic Cages: Architectures and Functions. *Chem. Rev.* **2014**, *114*, 8542−8578. (d) Paolesse, R.; Nardis, S.; Monti, D.; Stefanelli, M.; Di Natale, C. Porphyrinoids for Chemical Sensor Applications. *Chem. Rev.* **2017**, *117*, 2517−2583. (e) Akine, S. Control of guest binding behavior of metal-containing host molecules by ligand exchange. *Dalton Trans.* **2021**, *50*, 4429−4444.

(10) (a) Ayabe, M.; Ikeda, A.; Shinkai, S.; Sakamoto, S.; Yamaguchi, K. A novel [60]fullerene receptor with a Pd(II)-switched bisporphyrin cleft. *Chem. Commun.* **2002**, 1032−1033. (b) Linke-Schaetzel, M.; Anson, C. E.; Powell, A. K.; Buth, G.; Palomares, E.; Durrant, J. D.; Silviu Balaban, T.; Lehn, J.-M. Dynamic Chemical Devices: Photoinduced Electron Transfer and Its Ion-Triggered Switching in Nanomechanical Butterfly-Type Bis(porphyrin)terpyridines. *Chem. − Eur. J.* **2006**, *12*, 1931−1940. (c) Frey, J.; Tock, C.; Collin, J.-P.; Heitz, V.; Sauvage, J.-P. A [3]Rotaxane with Two Porphyrinic Plates Acting as an Adaptable Receptor. *J. Am. Chem. Soc.* **2008**, *130*, 4592−4593. (d) Kocher, L.; Durot, S.; Heitz, V. Control of the cavity size of flexible covalent cages by silver coordination to the peripheral binding sites. *Chem. Commun.* **2015**, *51*, 13181−13184. (e) Djemili, R.; Kocher, L.; Durot, S.; Peuronen, A.; Rissanen, K.; Heitz, V. Positive Allosteric Control of Guests Encapsulation by Metal Binding to Covalent Porphyrin Cages. *Chem. − Eur. J.* **2018**, *25*, 1481−1487. (f) Goswami, A.; Paululat, T.; Schmittel, M. Switching Dual Catalysis without Molecular Switch: Using A Multicomponent Information System for Reversible Reconfiguration of Catalytic Machinery. *J. Am. Chem. Soc.* **2019**, *141*, 15656−15663.

(11) Oliveri, C. G.; Gianneschi, N. C.; Nguyen, S. T.; Mirkin, C. A.; Stern, C. L.; Wawrzak, Z.; Pink, M. Supramolecular Allosteric Cofacial Porphyrin Complexes. *J. Am. Chem. Soc.* **2006**, *128*, 16286−16296.

(12) (a) Yoon, H.; Lee, C.-H.; Jang, W.-D. Absolute Stereochemical Determination of Chiral Carboxylates Using an Achiral Molecular Tweezer. *Chem. − Eur. J.* **2012**, *18*, 12479−12486. (b) Lee, C.-H.; Yoon, H.; Jang, W.-D. Biindole-Bridged Porphyrin Dimer as Allosteric Molecular Tweezers. *Chem. − Eur. J.* **2009**, *15*, 9972−9976.

(13) Muraoka, T.; Kinbara, K.; Aida, T. Mechanical twisting of a guest by a photoresponsive host. *Nature* **2006**, *440*, 512−515.

(14) Iordache, A.; Retegan, M.; Thomas, F.; Royal, G.; Saint-Aman, E.; Bucher, C. Redox-Responsive Porphyrin-Based Molecular Tweezers. *Chem. − Eur. J.* **2012**, *18*, 7648−7653.

(15) Yi, H.; Niu, L.; Wang, S.; Liu, T.; Singh, A. K.; Lei, A. Visible-Light-Induced Acetalization of Aldehydes with Alcohols. *Org. Lett.* **2017**, *19*, 122−125.

(16) Hu, J.; Ward, J. S.; Chaumont, A.; Rissanen, K.; Vincent, J.-M.; Heitz, V.; Jacquot de Rouville, H.-P. A Bis-Acridinium Macrocycle as Multi-Responsive Receptor and Selective Phase-Transfer Agent of Perylene. *Angew. Chem., Int. Ed.* **2020**, *59*, 23206−23212.

(17) Lindsey, J. S.; Schreiman, I. C.; Hsu, H. C.; Kearney, P. C.; Marguerettaz, A. M. Rothemund and Adler-Longo Reactions Revisited: Synthesis of Tetraphenylporphyrins under Equilibrium Conditions. *J. Org. Chem.* **1987**, *52*, 827−836.

(18) Loading of an amount of Grubbs I catalyst above 10 mol% leads to the formation of a side product, namely the functionalized **4·PF₆** with styrene. This product results from the higher conjugation and consequently to higher stability than **1·2PF₆**.

(19) The bis(acridinium-Zn(II) porphyrin) tweezer **1·2PF₆** was obtained as a trans isomer since no detectable peaks corresponding to the cis isomer were observed in the ¹H NMR spectrum.

(20) Stake, A.; Kobuke, Y. Dynamic supramolecular porphyrin systems. *Tetrahedron* **2005**, *61*, 13−41.

(21) Titration curves were fitted to a 1:2 model. Values for K_{11} of approximately $1.8\ (\pm0.1)\times10^5$ L mol^{-1} and for $K_{11\to12}$ of 799 ± 130 L mol^{-1} were estimated. At 1×10^{-3} mol L^{-1}, this corresponds to 87% of the 1:1 host-guest complex.

(22) Titration curves were fitted to a 1:2 model giving estimated binding constants of $K_{11}=1.4\ (\pm0.3)\times10^5$ and $K_{11\to12}=870\pm200$ L mol^{-1}.

(23) Altman, N. S. *An Introduction to Kernel and Nearest-Neighbor Nonparametric Regression*; The American Statistician, 1992, *46*, 175−185.

(24) Sneha, P.; George, P. D. C. Chapter Seven - Molecular Dynamics: New Frontier in Personalized Medicine. *Adv. Protein Chem. Struct. Biol.* **2016**, *102*, 181−224.

(25) Serillon, D.; Bo, C.; Barril, X. Testing automatic methods to predict free binding energy of host−guest complexes in SAMPL7 challenge. *J. Comput.-Aided Mol. Des.* **2021**, *35*, 209−222.

(26) The obtained value for the reduction potential of **1·2PF₆** is in agreement with the expected value for the 9-phenyl-N-methylacridinium motif ($E_{Red}=-0.54$ V vs SCE) (see Koper, N. W.; Jonker, S. A.; Verhoeven, J. W.; van Dijk, C. Electrochemistry of the 9-phenyl-10-methyl-acridan/acridinium redox system; a high-potential NADH/NAD$^+$ analogue. *Recl. Trav. Chim. Pays-Bas* **1985**, *104*, 296−302.

(27) Kadish, K.M. The Electrochemistry of Metalloporphyrins in nonaqueous media. *Progress in Inorganic Chemistry*, *34* (Ed.); John Wiley & Sons, Inc: New York, NY 1986, 435−605.

(28) Deans, R.; Niemz, A.; Breinlinger, E. C.; Rotello, V. M. Electrochemical Control of Recognition Processes. A Three-Component Molecular Switch. *J. Am. Chem. Soc.* **1997**, *119*, 10863−10864.

(29) Fajer, J.; Borg, D. C.; Forman, A.; Dolphin, D.; Felton, R. H. p-Cation radicals and dications of metalloporphyrins. *J. Am. Chem. Soc.* **1970**, *92*, 3451−3459.

(30) The same experiment in CH₂Cl₂ did not evidence emission in the NIR region. This can be explained by the red-shift and quenching of the CT band expected in the more polar solvent (see: (31b))

(31) (a) Armaroli, N.; Marconi, G.; Echegoyen, L.; Bourgeois, J.-P.; Diederich, F. Charge-Transfer Interactions in Face-to-Face Porphyrin-Fullerene Systems: Solvent-Dependent Luminescence in the Infrared Spectral Region. *Chem. − Eur. J.* **2000**, *6*, 1629−1645. (b) Armaroli, N.; Accorsi, G.; Song, F.; Palkar, A.; Echegoyen, L.; Bonifazi, D.; Diederich, F. Photophysical and Electrochemical Properties of meso,meso-Linked Oligoporphyrin Rods with Appended Fullerene Terminals. *ChemPhysChem* **2005**, *6*, 732−743.

(32) Nakajima, S.; Osuka, S. Synthesis of a Tetrakis(9-Anthryl) Substituted Porphyrin and Intramolecular Charge-Transfer Emission in its Dication. *Tetrahedron Lett.* **1995**, *36*, 8457−8460.

(33) Kamioka, K.; Cormier, R. A.; Lutton, T. W.; Connolly, J. S. Charge-Transfer Emission in Meso-Linked ZincPorphyrin-Anthraquinone Molecules. *J. Am. Chem. Soc.* **1992**, *14*, 4414−4415.

📖 Recommended by ACS

β,β-Directly Linked Porphyrin Rings: Synthesis, Photophysical Properties, and Fullerene Binding

Qiang Chen, Harry L. Anderson, *et al.*

MAY 18, 2023
JOURNAL OF THE AMERICAN CHEMICAL SOCIETY   READ 🗗

Secondary Bracing Ligands Drive Heteroleptic Cuboctahedral Pd^{II}_{12} Cage Formation

Carles Fuertes Espinosa, Jonathan R. Nitschke, *et al.*

APRIL 28, 2023
JOURNAL OF THE AMERICAN CHEMICAL SOCIETY   READ 🗗

Reversible Macrocycle-to-Macrocycle Interconversion Driven by Solvent Selection

Fei Wang, Qing He, *et al.*

MAY 12, 2023
JOURNAL OF THE AMERICAN CHEMICAL SOCIETY   READ 🗗

The Intracavity Extension of 28-Hetero-2,7-naphthiporphyrins in Reactions with Alkylamines

Katarzyna Ślusarek, Bartosz Szyszko, *et al.*

JUNE 22, 2023
ORGANIC LETTERS   READ 🗗

Get More Suggestions >